



Title	Extran ammary Paget's disease patient-derived xenografts harboring ERBB2 S310F mutation show sensitivity to HER2-targeted therapies
Author(s)	Maeda T, Akuya K, Itamura S, Shinya N, Ishihara H, Hiroshi Y, Anagi T, Teruki
Citation	Oncogene 39(5867-5875) <a href="https://doi.org/10.1038/s41388-020-1404-x">https://doi.org/10.1038/s41388-020-1404-x</a>
Issue Date	2020-09-03
Doc URL	<a href="http://hdl.handle.net/2115/80541">http://hdl.handle.net/2115/80541</a>
Type	article (author version)
Additional Information	There are other files related to this item in HUSCAP. Check the above URL.
File Information	Oncogene 39(5867).pdf



[Instructions for use](#)

1 ***Oncogene* ONC-2020-01144 Revised Version R1**

2 **Extramammary Paget's disease patient-derived xenografts harboring ERBB2**

3 **S310F mutation show sensitivity to HER2-targeted therapies**

4 Takuya Maeda<sup>1¶</sup>, Shinya Kitamura<sup>1¶</sup>, Hiroshi Nishihara<sup>2</sup>, Teruki Yanagi<sup>1\*</sup>

5 <sup>1</sup> *Department of Dermatology, Faculty of Medicine and Graduate School of Medicine,*

6 *Hokkaido University, Sapporo, Japan*

7 <sup>2</sup> *Genomics Unit, Keio Cancer Center, Keio University School of Medicine, Tokyo,*

8 *Japan*

9

10 \*Correspondence to Teruki Yanagi, M.D., Ph.D.

11 *Department of Dermatology, Faculty of Medicine and Graduate School of Medicine,*

12 *Hokkaido University, N15 W7, Kita-ku, Sapporo 060-8638, Japan*

13 Telephone: +81-11-706-7387

14 Facsimile: +81-11-706-7820

15 E-mail: [yanagi@med.hokudai.ac.jp](mailto:yanagi@med.hokudai.ac.jp)

16

17 <sup>¶</sup>These authors contributed equally to this work.

18

19 Word count: 200-word abstract, 2899-word text

20 References: 39

21 Tables: 0

22 Figures: 5

23 Supplementary figures: 7

24 Supplementary tables: 2

25

26 Running title: A novel experiment model for extramammary Paget's disease

27

28 Abbreviations:

29 EMPD: extramammary Paget's disease

30 G: generation

31 HE: hematoxylin and eosin

32 LOH: loss of heterozygosity

33 PDX: patient-derived xenograft

34 TUNEL: terminal deoxynucleotidyl transferase dUTP nick end labeling

35 VAF: variant allele frequency

36

37

38 **Abstract**

39 Although the prognosis of advanced extramammary Paget's disease (EMPD) is poor,  
40 there have been no preclinical research models for the development of novel  
41 therapeutics. This study aims to establish a preclinical research model for EMPD. We  
42 transplanted EMPD tissue into immunodeficient NOD/Scid mice. Histopathological and  
43 genetic analyses using a comprehensive cancer panel were performed. For *in vivo*  
44 preclinical treatments, trastuzumab, lapatinib, docetaxel, or eribulin were administered  
45 to patient-derived xenograft (PDX) models. Tissue transplanted from the EMPD patient  
46 was enlarged in NOD/Scid mice and was transplanted into further generations. Both the  
47 transplantation of PDX into *nu/nu* mice and the reanimation of the cryopreserved  
48 xenografted tumors in NOD/Scid mice were successful. We also established an EMPD-  
49 PDX-derived primary cell culture. Histopathologically, the xenografted tumors were  
50 positive for CK7, which was consistent with the patient's tumors. Genetically, the  
51 pathogenic mutation *ERBB2* S310F was detected in the patient's tumors (primary  
52 intraepidermal lesion, metastatic lymph node) and was observed in the xenografted  
53 tumors even after continued passages. The xenografted tumors responded well to  
54 trastuzumab and lapatinib therapy. Also, cytotoxic agents (docetaxel and eribulin) were  
55 effective against the xenografted tumors. This PDX model (EMPD-PDX-H1) could be a  
56 powerful tool for the research and development of EMPD treatments.

57 **Introduction**

58 Paget's disease is a rare adnexal neoplasm that was first described by Sir James Paget in  
59 1874 (ref. 1). Extramammary Paget's disease (EMPD) is a variant that is commonly  
60 seen in the genital areas and anus among the senior population (ref. 2), and the number  
61 of cases has been increasing in recent years (ref. 3). In most EMPD cases, tumor cells  
62 are localized in the epidermis, and the prognosis is relatively favourable (ref. 4).  
63 However, once tumor cells invade the dermis, patients are at a risk of lymph node and  
64 visceral metastases, and the prognosis becomes significantly poorer (ref. 5-7). A multi-  
65 center retrospective study by Ohara et al. showed that the 5-year survival rate for EMPD  
66 patients with distant metastasis was only 7% (ref. 7). There have been several  
67 retrospective studies on treatments for metastatic EMPD, such as cytotoxic  
68 chemotherapies (ref. 8-12), and small molecular inhibitors (ref. 13-15). However, the  
69 efficacies of these treatments have been evaluated only in single case reports or case  
70 series containing small numbers of patients. Thus, the development of novel therapeutic  
71 strategy for advanced EMPD has been desired.

72 In recent years, the usefulness of patient-derived xenograft (PDX) models has  
73 been reported in many types of cancers (ref. 16-18). PDX models have demonstrated an  
74 ability to maintain the characteristics of the original tumor and to be useful for  
75 preclinical therapeutic studies in certain cancers. These models have shown to be

76 predictive of clinical outcomes and are being used for preclinical drug evaluation,  
77 biomarker identification, biological studies, and personalized medicine strategies (ref.  
78 17). For EMPD, Nishi et al. reported the first PDX model using an EMPD tumor in  
79 1992 (ref. 19). They transplanted metastatic EMPD tissue into nude mice (*nu/nu* mice).  
80 Reportedly, their xenografted tumor maintained the histopathological features of the  
81 patient's original tumor, and they investigated the effect of hormonal stimulation on  
82 tumor growth. To the best of our knowledge, no additional studies using this PDX  
83 model have been published. Thus, no preclinical research models of EMPD including  
84 cell lines and PDX are currently available.

85           Here, we report a novel PDX model of EMPD (EMPD-PDX-H1) harboring a  
86 pathogenic *ERBB2* mutation. We performed histopathological and genetic analyses to  
87 confirm that the xenografted tumors maintained the characteristics of the patient's  
88 original tumors. Further, we performed treatment experiments using cytotoxic agents  
89 and HER2-targeted therapies.

90 **Results**

91 **Establishment of the EMPD-PDX-H1**

92 A schematic of the present study is shown in Figure 1. To establish a patient-derived  
93 EMPD xenograft, surgically resected tissue was transplanted onto the flanks of  
94 NOD/Scid mice (Figure 2 A, B). The transplanted EMPD tumor tissue grew into a firm  
95 nodule of more than 10 mm in diameter over the course of 5 months (generation 0: G0,  
96 Figure 2C). The xenograft tissue was analyzed by HE staining and  
97 immunohistochemistry for CK7 and HER2, and for androgen, estrogen and  
98 progesterone receptors. The EMPD-PDX-H1 tissue exhibited similar morphology and  
99 protein expressions to those of the patient's tissues (primary tumor and metastatic  
100 lymph node) (Figure 2D and Supplementary Figure S1). Once the tumor volume  
101 reached 500–1000 mm<sup>3</sup>, the EMPD-PDX-H1 tumors were transplanted into the next  
102 generation of NOD/Scid mice. By the third passage, the growth volume curve of PDX  
103 in each generation became stable (Supplementary Figure S2). Also, we transplanted  
104 EMPD-PDX-H1 tumors into *nu/nu* mice. Both the transplantation of EMPD-PDX-H1  
105 tumors into the *nu/nu* mice (3/3, 100%) and the reanimation of the cryopreserved  
106 EMPD-PDX-H1 tumors in the NOD/Scid mice (10/12, 83.3 %) were successful  
107 (Supplementary Figure S3 and S4). Also, we established primary culture cells from the  
108 3<sup>rd</sup> generation of EMPD-PDX-H1, in which cultured tumor cells were round or cuboidal

109 (Supplementary Figure S5).

110

111 **EMPD-PDX-H1 harbors an *ERBB2* S310F mutation identical to that of the**  
112 **patient's tumors**

113 To investigate the characteristics of EMPD-PDX-H1 and the similarity between the  
114 patient's tissues (primary tumor and metastatic lymph node) and EMPD-PDX-H1, we  
115 performed gene mutation analysis. To compare the cancer-associated genomic profile of  
116 the patient's tumors to those of their corresponding xenografts, we performed deep  
117 sequencing using a comprehensive cancer panel. EMPD-PDX-H1 tumors faithfully  
118 maintained the pathogenic genomic DNA alterations of *ERBB2* (c.929C>T, p.S310F),  
119 which was observed in the corresponding tumor (metastatic lymph node) of the patient  
120 (Figure 3A). *ERBB2* S310F mutation was conserved even after continued passages of  
121 EMPD-PDX-H1 (Figure 3A, PDX (G2)). Sanger sequencing targeting *ERBB2* mutation  
122 revealed that the patient's primary tumor (resected 12 years earlier) harbored the  
123 identical *ERBB2* S310F mutation (Figure 3B).

124 In addition to *ERBB2* S310F being retained in EMPD-PDX-H1, so were *TP53*  
125 A161T and *RBI* S780\*. In the patient's lymph nodes, the variant allele frequency (VAF)  
126 for *TP53* A161T was 50.4% and for *RBI* S780\* was 42.5%. The VAF of both mutations  
127 in EMPD-PDX-H1 was elevated to 100% (Supplementary Table S1). This is because



128 the normal allele was lost and the proportion of normal cells decreased in EMPD-PDX-  
129 H1 tumor. The mutation of *NF1* D2545N was also retained in EMPD-PDX-H1;  
130 however, its VAFs (47.5% in G1 and 50.3% in G2) suggest that the normal allele was  
131 sustained. *NOTCH1* S1409N has been observed in EMPD-PDX-H1 tumors (G1 and  
132 G2) with high VAF, possibly due to the loss of heterozygosity (LOH). Since no such  
133 mutation was detected in the patient's tumor, it might be crucial for PDX implantation.

134

### 135 **Treatment experiments using EMPD-PDX-H1**

136 Preclinical studies for EMPD have not been reported until this paper, possibly due to the  
137 unavailability of EMPD cell lines/PDX tissues. We performed treatment experiments to  
138 investigate whether EMPD-PDX-H1 responds to targeted therapies and chemotherapies  
139 as reported in clinical settings (Ref. 8-15). For the targeted therapy, since the PDX  
140 harbored pathogenic *ERBB2* S310F, we treated the tumor with HER2-targeted therapies  
141 (trastuzumab, lapatinib, and combination of the two). The single use of trastuzumab or  
142 lapatinib was found to suppress tumor progression, but the combined therapy was found  
143 to remarkably inhibit tumor growth (Figure 4, A–F). Regarding cytotoxic  
144 chemotherapies, the xenografted model responded well to docetaxel (Figure 5, A, B),  
145 which is reported to be effective against metastatic EMPD (Ref. 10, 11). We tested  
146 eribulin monotherapy, which has been shown to be effective as a second-line treatment

147 for breast cancer (ref. 20). Eribulin therapies (1.5 mg/kg/week) eliminated EMPD-PDX-  
148 H1 completely, and no relapse was observed for one week (Figure 5 C, D). We  
149 administered 0.45 mg/kg/week eribulin and obtained similar results (Figure 5 E, F). The  
150 results of treatment experiments were also confirmed by Ki-67 staining and terminal  
151 deoxynucleotidyl transferase dUTP nick end labeling (TUNEL) assays. In Ki-67  
152 staining, all of the treated EMPD-PDX-H1 tumors showed a significantly lower ratio of  
153 positive cells than the non-treated tumors showed (Supplementary Figure S6). In the  
154 TUNEL assays, all of the treated EMPD-PDX-H1 tumors showed a significantly higher  
155 ratio of TUNEL-positive tumor cells than the control tumor cells showed  
156 (Supplementary Figure S7).

157

158 **Discussion**

159 The present study presented an EMPD PDX model that reproduced the patient's original  
160 tumor morphologically and genetically. We also reported the promising potency of  
161 HER-2 targeted therapies and cytotoxic chemotherapies.

162 It has been reported that certain EMPD cases revealed overexpression of HER2  
163 as assessed by immunohistochemistry and *in situ* hybridization (ref. 21-23). In addition,  
164 somatic mutations analyses of EMPD have detected *ERBB2* mutations (ref. 24, 25).  
165 Overexpression of HER2 protein and *ERBB2* gene amplification positively correlate  
166 with disease progression (ref. 22). Clinically, several case reports have shown the  
167 efficacy of HER2-targeted therapies such as lapatinib and trastuzumab against  
168 metastatic EMPD (ref.13-15). In light of these facts, the HER2 signalling pathway is  
169 considered to contribute to carcinogenesis in HER2-positive/mutated EMPD. In the  
170 present study, the PDX model was found to harbor a pathogenic *ERBB2* mutation  
171 (S310F) without definitive amplification. *ERBB2* S310F mutation corresponds to the  
172 extracellular domain of ERBB2/HER2, and that domain has been reported as having the  
173 most common mutation of *ERBB2* in various cancers such as breast, lung, bladder, and  
174 colon (ref. 26). Greulich et al. reported that *ERBB2* S310F mutation leads to  
175 ERBB2/HER2 activation via two distinct mechanisms, characterized by elevated C-  
176 terminal tail phosphorylation or by covalent dimerization through intermolecular

177 disulfide bond formation (ref. 27). The S310F mutation has been reported in *ERBB2*  
178 non-amplified breast cancer and is not necessarily accompanied by *ERBB2*  
179 amplification (ref. 28). Also, HER2-targeted therapy is effective against lung, colon, and  
180 other cancers harboring the S310F mutation (ref. 27, 29, 30). Concerning EMPD,  
181 Mishra et al. were the first to report a case of EMPD harboring the *ERBB2* S310F  
182 mutation in which trastuzumab and capecitabine combination therapy was remarkably  
183 effective against multiple metastatic lesions (ref. 15). This case report is consistent with  
184 our experimental results showing that EMPD-PDX-H1 harboring *ERBB2* S310F is  
185 sensitive to HER2-targeted therapies. In addition, a phase 2 clinical study using  
186 trastuzumab combined with docetaxel for HER2-positive EMPD (UMIN000021311) is  
187 under way at Keio University in Japan.

188         The present study has also demonstrated the antitumor effects of cytotoxic  
189 chemotherapies. We herein tried the administration of eribulin, an inhibitor of  
190 microtubule dynamics that has proven effective against breast cancer (ref. 20, 31), since  
191 recent studies suggest that EMPD and mammary Paget's disease (a breast cancer)  
192 harbor common recurrent mutations (ref 24, 32). The eribulin administration showed  
193 high efficacy against all of EMPD-PDX-H1 tumors. Although there are no clinical  
194 reports of eribulin being effective against EMPD-PDX-H1, it is suggested that eribulin  
195 may be a treatment option for EMPD.

196           Unfortunately, we established the EMPD-PDX from only one patient in the  
197 present study due to the small number of advanced EMPD cases. In the future, it is  
198 necessary to confirm whether PDX models can be established from other patients using  
199 the same methods and to conduct treatment experiments on other PDX models to  
200 develop preclinical studies. Despite this limitation, EMPD-PDX-H1 is the first to  
201 investigate the efficacy of antitumor agents and to help in the search for new treatments  
202 for advanced EMPD.

203           In summary, we generated a novel EMPD PDX model that maintained the  
204 original patient's tumors both histopathologically and genetically. Our therapeutic  
205 experiments revealed *in vivo* tumor growth inhibition by anti-HER2 therapies (lapatinib  
206 and trastuzumab) and cytotoxic agents (docetaxel and eribulin). EMPD-PDX-H1 could  
207 be useful for developing effective therapies for EMPD.

208

209 **Materials and Methods**

210 **Samples from the EMPD patient**

211 EMPD tissues were obtained from inguinal lymph node metastases of a 78-year-old  
212 Japanese female whose primary genital skin lesion had been removed 12 years before  
213 the lymph node metastasis occurred (Figure 2 A, B). She had no significant familial or  
214 past medical history. The resected metastatic lymph node was separated into two parts:  
215 One was immediately transported on ice for transplantation, and the other was fixed in  
216 formalin and embedded into paraffin for pathological diagnosis. Written informed  
217 consent was obtained from the patient, and this research was approved by the Ethics  
218 Committee of Hokkaido University Hospital in accordance with the Declaration of  
219 Helsinki (IRB approval number: 018-0424).

220

221 **Establishment of EMPD-PDX-H1**

222 A 10-mm-wide piece of EMPD tissue was subcutaneously transplanted with Matrigel  
223 (BD Bioscience, Franklin Lakes, NJ, USA) onto both flanks of a 5-week-old female  
224 NOD/Scid mouse (Clea, Tokyo, Japan). The mice in this study were housed in a specific  
225 pathogen-free condition at a fixed temperature (22–25°C) and were held on a 12-hour  
226 light-dark cycle. The mice were given distilled water and standard chow *ad libitum*.  
227 Animal use procedures were approved by the institutional committee of Hokkaido

228 University (approval numbers 19-0015 and 19-0093). The tumor-transplanted mouse  
229 was observed twice a week for 5 months. The tumors were measured once a week by  
230 caliper. Tumor volume was calculated using the following formula: (long axis x short  
231 axis<sup>2</sup>)/2 (ref. 33). Once the tumor volume reached 500–1000 mm<sup>3</sup>, EMPD-PDX-H1  
232 tumors were transplanted into the next generation of NOD/Scid mice. In the first two  
233 consecutive mouse-to-mouse passages, EMPD-PDX-H1 tumors were separated into  
234 three sections: The first part was cut into pieces (less than 5 mm in diameter) for  
235 transplantation, and the second part was frozen immediately at –80 °C for DNA  
236 extraction and was fixed in formalin and then embedded into paraffin for pathological  
237 analysis. Treatment experiments were performed on the 3<sup>rd</sup>–5<sup>th</sup> generations. At the 4<sup>th</sup>  
238 passage, transplantation was also performed on 5-week-old female nude (*nu/nu*) mice  
239 (Clea, Tokyo, Japan). Greater amounts of fresh tumor pieces at passages 4 and 5 were  
240 frozen in CryoStor<sup>®</sup> CS10 (BioLife Solutions, Owego, NY, USA) and stored at –80 °C  
241 (ref. 34). The cryopreserved EMPD-PDX-H1 tumors were re-transplanted into  
242 NOD/Scid mice to confirm reanimation.

243

#### 244 **Histopathological analyses**

245 Formalin-fixed, paraffin-embedded tissue sections of the patient's tumors or the  
246 xenografted tumors were cut into 4- $\mu$ m sections. Hematoxylin and eosin (HE) staining

247 as well as immunohistochemistry for CK7 (Dako, Code. M7018, Denmark), HER2  
248 (Dako, Code. A0485, Denmark), androgen receptor (ScyTek laboratories, RA0012-C,  
249 USA), estrogen receptor (Leica Biosystems, NCL-L-6F11, UK), progesterone receptor  
250 (Leica Biosystems, NCL-L-PGR-312, UK) and Ki-67 (Abcam, #ab8191) were  
251 performed to compare the histopathology of the primary lesions, metastatic lymph  
252 nodes, and xenografts. DAB chromogen was applied to yield a brown color (ref. 35).  
253 For nuclear Ki-67 expression, the percentage of positive cells among at least 100 cancer  
254 cells from three randomly selected fields of vision using a high-power lens (x 400) were  
255 calculated. The expression levels of HER2 protein were evaluated according to the  
256 HER2 testing guideline for breast cancer as follows (ref. 36).  
257 3+: “circumferential membrane staining that is complete, intense”  
258 2+: “circumferential membrane staining that is incomplete and/or weak to moderate and  
259 within > 10% of the invasive tumor cells or complete and circumferential membrane  
260 staining that is intense and within  $\leq$  10% of the invasive tumor cells”  
261 1+: “incomplete membrane staining that is faint or barely perceptible and within > 10%  
262 of the invasive tumor cells”  
263 0: “no staining observed or membrane staining that is incomplete and is faint or barely  
264 perceptible and within  $\leq$  10% of the invasive tumor cells”  
265



266 **TUNEL assays**

267 Cell death was assessed by the TUNEL method using an In Situ Cell Death Detection  
268 Kit (Roche, #11684817910) according to the manufacturer's instructions. For nuclear  
269 TUNEL staining, the percentage of positive cells among at least 100 cancer cells from  
270 three randomly selected fields of vision using a high-power lens (x 400) was calculated.

271

272 **Gene mutation analysis**

273 EMPD patient tissues and EMPD-PDX-H1 tissues were pathologically reviewed to  
274 ensure that the tumor cell content was high enough and that no significant tumor  
275 necrosis had occurred before DNA extraction. Genomic DNA was extracted from our  
276 patient's blood and from each tissue sample using the DNA Mini Kit (QIAGEN,  
277 Cat#51304, Germany) or the GeneRead FFPE DNA Kit (QIAGEN, Cat#180134,  
278 Germany). The quantity and purity of DNA samples were measured using a Nanodrop  
279 ND-1000 UV/VIS Spectrophotometer (Thermo Scientific, USA). DNA fragment  
280 integrity was confirmed by electrophoresis using 1% agarose gel. The concentrations of  
281 DNA samples were normalized to 20 ng/ $\mu$ l, and those samples were stored at  $-20^{\circ}\text{C}$   
282 until use. Genomic testing was performed at the genomic unit of the Keio Cancer Center  
283 in Tokyo, Japan. After the quality of the DNA was checked based on the DNA integrity  
284 number (DIN) score calculated using the Agilent 2000 TapeStation (Agilent

285 Technologies, Waldbronn, Germany), targeted amplicon exome sequencing for 160  
286 cancer-related genes was performed using the Illumina MiSeq sequencing platform  
287 (Illumina, San Diego, CA). The list of 160 cancer-related genes included in the  
288 comprehensive cancer panel is shown in Supplementary Table S2. The minimum  
289 amount of DNA was 50 ng, and the minimum quality for DNA was that with a DIN  
290 score over 3.1. The sequencing data were analyzed using an original bioinformatics  
291 pipeline called GenomeJack (Mitsubishi Space Software, Tokyo, Japan). In addition, we  
292 performed mutation analysis by Sanger sequencing to confirm the pathogenic *ERBB2*  
293 gene alteration in the primary lesions using the following primers: forward primer 5'-  
294 CGGTAATGCTGCTCATGGTG-3' and reverse primer 5'-  
295 CTTGCTGCACTTCTCACACC-3'.

296

### 297 **EMPD-PDX-H1-derived primary cell culture**

298 Tumor tissue from EMPD-PDX-H1 mice (3<sup>rd</sup> generation) was minced and washed with  
299 PBS repeatedly. The minced tissue was directly plated onto dishes coated with type I  
300 collagen (Iwaki, Tokyo, Japan) in a medium of RPMI (Nakalai, Kyoto, Japan)  
301 containing 10% fetal bovine serum (FBS, Sigma).

302

### 303 **Treatment experiments using EMPD-PDX-H1**

304 Tumor growth curves for all EMPD-PDX-H1 were generated using the kinetic  
305 measurement of tumor volumes. The tumor volume range of 50 to 100 mm<sup>3</sup> in the  
306 tumor-bearing NOD/Scid mice was randomized, and treatment experiments were begun.  
307 All treatment experiments were performed with a minimum of n = 4 mice per condition.  
308 Control mice were administered with 100 µl of 0.5% hydroxypropyl methylcellulose  
309 once a day orally (n = 5), intraperitoneally injected with 100 µl of PBS twice per week  
310 (n = 5), or intravenously injected with 100 µl of PBS once per week (n = 5). In the  
311 HER2-targeted treatments, trastuzumab (10 mg/kg, Herceptin®, Chugai Pharmaceutical  
312 Co., Ltd., Tokyo, Japan) was given intraperitoneally twice weekly according to a  
313 previous study (ref. 37). Lapatinib (100 mg/kg, CS-0036, Chem Scene, USA) was  
314 administered once a day orally in 0.5% hydroxypropyl methylcellulose and 0.1% Tween  
315 80 (P1754, Sigma-Aldrich, Germany) (ref. 38). We also administered trastuzumab and  
316 lapatinib in combination (ref. 37). Concerning cytotoxic agents, docetaxel (20 mg/kg,  
317 Santa Cruz Biotechnology, CA, USA, #sc-201436) and eribulin (1.5 or 0.45 mg/kg,  
318 Halaven, Eisai Co., Ltd., Tokyo, Japan) were administered intravenously once per week  
319 (ref. 31, 39). Tumor volumes were measured once a week by caliper, and tumor weights  
320 were measured with a scale at 28 days after treatment initiation. Tumor volume and  
321 weight were recorded in a blinded manner.  
322

323 **Statistical analysis**

324 To evaluate the statistical significance of the treatment experiments, Student's *t*-test was  
325 used to compare tumor volume between the treatment groups and the control group.

326 Statistical tests were two sided, with  $P < 0.05$  considered significant.

327

328 **Disclosure of Potential Conflicts of Interest**

329 None to declare.

330

331 **Acknowledgments**

332 We thank Ms. Yuko Tateda for her technical assistance. This work was supported in part  
333 by KAKENHI grant #18K08259 to T. Yanagi from the Ministry of Education, Culture,  
334 Sports, Science and Technology in Japan.

335

336 **References**

- 337 1. Paget SJ. On disease of the mammary areola preceding cancer of the mammary  
338 gland. *St. Bartholomew's Hosp Rep.* 1874; 10:87–9.
- 339 2. Kanitakis J. Mammary and extramammary Paget's disease. *J Eur Acad*  
340 *Dermatol Venereol.* 2007; 21:581–90.
- 341 3. Herrel LA, Weiss AD, Goodman M, Johnson TV, Osunkoya AO, Delman KA,  
342 et al. Extramammary Paget's disease in males: survival outcomes in 495  
343 patients. *Ann Surg Oncol.* 2015; 22:1625–30.
- 344 4. Karam A, Dorigo O. Treatment outcomes in a large cohort of patients with  
345 invasive Extramammary Paget's disease. *Gynecol Oncol.* 2012; 125:346–51.
- 346 5. Hatta N, Yamada M, Hirano T, Fujimoto A, Morita R. Extramammary Paget's  
347 disease: treatment, prognostic factors and outcome in 76 patients. *Br J*  
348 *Dermatol.* 2008; 158:313–8.
- 349 6. Hirakawa S, Detmar M, Kerjaschki D, Nagamatsu S, Matsuo K, Tanemura A,  
350 et al. Nodal lymphangiogenesis and metastasis: Role of tumor-induced  
351 lymphatic vessel activation in extramammary Paget's disease. *Am J Pathol.*  
352 2009; 175:2235–48.
- 353 7. Ohara K, Fujisawa Y, Yoshino K, Kiyohara Y, Kadono T, Murata Y, et al. A  
354 proposal for a TNM staging system for extramammary Paget disease:

- 355 Retrospective analysis of 301 patients with invasive primary tumors. J  
356 Dermatol Sci. 2016 Sep;83(3):234–9.
- 357 8. Oashi K, Tsutsumida A, Namikawa K, Tanaka R, Omata W, Yamamoto Y, et al.  
358 Combination chemotherapy for metastatic extramammary Paget disease. Br J  
359 Dermatol. 2014; 170:1354–7.
- 360 9. Tokuda Y, Arakura F, Uhara H. Combination chemotherapy of low-dose 5-  
361 fluorouracil and cisplatin for advanced extramammary Paget's disease. Int J  
362 Clin Oncol. 2015; 20:194–7.
- 363 10. Yoshino K, Fujisawa Y, Kiyohara Y, Kadono T, Murata Y, Uhara H, et al.  
364 Usefulness of docetaxel as first-line chemotherapy for metastatic  
365 extramammary Paget's disease. J Dermatol. 2016; 43:633–7.
- 366 11. Kato M, Yoshino K, Maeda T, Nagai K, Oaku S, Hiura A, et al. Single-agent  
367 taxane is useful in palliative chemotherapy for advanced extramammary  
368 Paget's disease; A Case Series. Br J Dermatol. 2019; 181:831–2.
- 369 12. Hirai I, Tanese K, Nakamura Y, Ishii M, Kawakami Y, Funakoshi T.  
370 Combination Cisplatin-Epirubicin-Paclitaxel Therapy for Metastatic  
371 Extramammary Paget's Disease. Oncologist. 2019; 24:e394–6.
- 372 13. Karam A, Berek JS, Stenson A, Rao J, Dorigo O. HER-2/neu targeting for  
373 recurrent vulvar Paget's disease: a case report and literature review. Gynecol

- 374 Oncol. 2008; 111:568–71.
- 375 14. Takahagi S, Noda H, Kamegashira A, et al. Metastatic extramammary Paget's  
376 disease treated with paclitaxel and trastuzumab combination chemotherapy. *J*  
377 *Dermatol.* 2009 36:457–61.
- 378 15. Vornicova O, Hershkovitz D, Yablonski-Peretz T, Ben-Itzhak O, Keidar Z, Bar-  
379 Sela G. Treatment of metastatic extramammary Paget's disease associated with  
380 adnexal adenocarcinoma, with anti-HER2 drugs based on genomic alteration  
381 ERBB2 S310F. *Oncologist.* 2014; 19:1006–7.
- 382 16. Bertotti A, Migliardi G, Galimi F, Sassi F, Torti D, Isella C, et al. A molecularly  
383 annotated platform of patient-derived xenografts ("xenopatiens") identifies  
384 HER2 as an effective therapeutic target in cetuximab-resistant colorectal  
385 cancer. *Cancer Discov.* 2011; 1:508–23.
- 386 17. Hidalgo M, Amant F, Biankin AV, Budinská E, Byrne AT, Caldas C, et al.  
387 Patient-derived xenograft models: an emerging platform for translational  
388 cancer research. *Cancer Discov.* 2014; 4:998–1013.
- 389 18. Koga Y, Ochiai A. Systematic Review of Patient-Derived Xenograft Models for  
390 Preclinical Studies of Anti-Cancer Drugs in Solid Tumors. *Cells.* 2019; 8:E418.
- 391 19. Nishi M, Tashiro M, Yoshida H. Stimulation of growth by both androgen and  
392 estrogen of the EMP-K1 transplantable tumor with androgen and estrogen



- 393 receptors from human extramammary Paget's disease in nude mice. *J Natl*  
394 *Cancer Inst.* 1992; 84:519–23.
- 395 20. Twelves C, Cortes J, Vahdat L, Olivo M, He Y, Kaufman PA, et al. Efficacy of  
396 eribulin in women with metastatic breast cancer: a pooled analysis of two  
397 phase 3 studies. *Breast Cancer Res Treat.* 2014; 148:553–61.
- 398 21. Richter CE, Hui P, Buza N, Silasi DA, Azodi M, Santin AD, et al. HER-2/NEU  
399 overexpression in vulvar Paget disease: the Yale experience. *J Clin Pathol.*  
400 2010; 63:544–7.
- 401 22. Tanaka R, Sasajima Y, Tsuda H, Namikawa K, Tsutsumida A, Otsuka F, et al.  
402 Human epidermal growth factor receptor 2 protein overexpression and gene  
403 amplification in extramammary Paget disease. *Br J Dermatol.* 2013; 168:1259–  
404 66.
- 405 23. Tanaka R, Sasajima Y, Tsuda H, Namikawa K, Takahashi A, Tsutsumida A, et  
406 al. Concordance of the HER2 protein and gene status between primary and  
407 corresponding lymph node metastatic sites of extramammary Paget disease.  
408 *Clin Exp Metastasis.* 2016; 33:687–97.
- 409 24. Zhang G, Zhou S, Zhong W, Hong L, Wang Y, Lu S, et al. Whole-Exome  
410 Sequencing Reveals Frequent Mutations in Chromatin Remodeling Genes in  
411 Mammary and Extramammary Paget's Diseases. *J Invest Dermatol.* 2019;

412 139:789–795.

413 25. Kiniwa Y, Yasuda J, Saito S, Saito R, Motoike IN, Danjoh I, et al. Identification  
414 of genetic alterations in extramammary Paget disease using whole exome  
415 analysis. *J Dermatol Sci.* 2019; 94:229–235.

416 26. Tate JG, Bamford S, Jubb HC, Sondka Z, Beare DM, Bindal N, et al.  
417 COSMIC: the Catalogue Of Somatic Mutations In Cancer. *Nucleic Acids Res.*  
418 2019; 47:D941–7.

419 27. Greulich H, Kaplan B, Mertins P, Chen TH, Tanaka KE, Yun SH, et al.  
420 Functional analysis of receptor tyrosine kinase mutations in lung cancer  
421 identifies oncogenic extracellular domain mutations of ERBB2. *Proc Natl Acad*  
422 *Sci U S A.* 2012; 109:14476–81.

423 28. Ma CX, Bose R, Gao F, Freedman RA, Telli ML, Kimmick G, et al. Neratinib  
424 Efficacy and Circulating Tumor DNA Detection of HER2 Mutations in HER2  
425 Nonamplified Metastatic Breast Cancer. *Clin Cancer Res.* 2017; 23:5687–95.

426 29. Kavuri SM, Jain N, Galimi F, Cottino F, Leto SM, Migliardi G, et al. HER2  
427 activating mutations are targets for colorectal cancer treatment. *Cancer Discov.*  
428 2015; 5:832–41.

429 30. Hyman DM, Piha-Paul SA, Won H, Won H, Rodon J, Saura C, et al. HER  
430 kinase inhibition in patients with HER2- and HER3-mutant cancers. *Nature.*

- 431 2018; 554:189–194.
- 432 31. Towle MJ, Nomoto K, Asano M, Kishi Y, Yu MJ, Littlefield BA. Broad  
433 spectrum preclinical antitumor activity of eribulin (Halaven(R)): optimal  
434 effectiveness under intermittent dosing conditions. *Anticancer Res.* 2012;  
435 32:1611–9.
- 436 32. Takeichi T, Okuno Y, Matsumoto T, Tsunoda N, Suzuki K, Tanahashi K, et al.  
437 Frequent FOXA1-Activating Mutations in Extramammary Paget's Disease.  
438 *Cancers (Basel).* 2020; 12(4).
- 439 33. Yanagi T, Krajewska M, Matsuzawa S, Reed JC. PCTAIRE1 phosphorylates  
440 p27 and regulates mitosis in cancer cells. *Cancer Res* 2014; 74:5795–807.
- 441 34. Ivanics T, Bergquist JR, Liu G, Kim MP, Kang Y, Katz MH, et al. Patient-  
442 derived xenograft cryopreservation and reanimation outcomes are dependent on  
443 cryoprotectant type. *Lab Invest.* 2018; 98:947–956.
- 444 35. Yanagi T, Watanabe M, Hata H, Kitamura S, Imafuku K, Yanagi H, et al. Loss  
445 of TRIM29 Alters Keratin Distribution to Promote Cell Invasion in Squamous  
446 Cell Carcinoma. *Cancer Res.* 2018; 78:6795-6806.
- 447 36. Wolff AC, Hammond MEH, Allison KH, Harvey BE, Mangu PB, Bartlett JMS,  
448 et al. Human Epidermal Growth Factor Receptor 2 Testing in Breast Cancer:  
449 American Society of Clinical Oncology/College of American Pathologists

- 450 Clinical Practice Guideline Focused Update. *J Clin Oncol*. 2018; 36: 2105–22.
- 451 37. Wainberg ZA, Anghel A, Desai AJ, Ayala R, Luo T, Safran B, et al. Lapatinib, a  
452 dual EGFR and HER2 kinase inhibitor, selectively inhibits HER2-amplified  
453 human gastric cancer cells and is synergistic with trastuzumab in vitro and in  
454 vivo. *Clin Cancer Res*. 2010; 16:1509–19.
- 455 38. Nonagase Y, Yonesaka K, Kawakami H, Watanabe S, Haratani K, Takahama T,  
456 et al. Heregulin-expressing HER2-positive breast and gastric cancer exhibited  
457 heterogeneous susceptibility to the anti-HER2 agents lapatinib, trastuzumab  
458 and T-DM1. *Oncotarget*. 2016; 7:84860–71.
- 459 39. Hendrikx JJ, Lagas JS, Song JY, Rosing H, Schellens JHM, Beijnen JH, et al.  
460 Ritonavir inhibits intratumoral docetaxel metabolism and enhances docetaxel  
461 antitumor activity in an immunocompetent mouse breast cancer model. *Int J*  
462 *Cancer*. 2016; 138:758–69.
- 463

464 **Figure legends**

465 **Figure 1. Schematic of the study method**

466 Tissue obtained from the EMPD patient is transplanted into NOD/Scid mice (generation  
467 0: G0). The xenografted tumors are transplanted to further generations (G1-G4) and  
468 used for cell culture, histopathological analysis, genetic analysis, and treatment  
469 experiments.

470

471 **Figure 2. The clinical manifestations and immunohistopathological findings for the**  
472 **primary site, the metastatic lymph node, and EMPD-PDX-H1**

473 A, Clinical photo of the patient's primary tumor. B, Computed tomography image of the  
474 patient's lymph node metastasis (yellow arrow) and the clinical photo (inset). C,  
475 Appearance of the xenografted tumor on a NOD/Scid mouse (red arrowheads). D,  
476 Hematoxylin and eosin staining and immunohistochemistry of CK7 and HER2. The  
477 score for HER2 expression in invasive tumor cells was 1+, which is consistent with that  
478 in PDX tissue. Scale bar = 100  $\mu$ m.

479

480 **Figure 3. EMPD-PDX-H1 tumors harbor *ERBB2* gene mutations identical to those**  
481 **of the patient's primary and metastatic tumors.**

482 A, Actionable genetic alterations in the patient's samples and EMPD-PDX-H1 tumors  
483 through deep sequencing using a comprehensive cancer panel. Identical gene alterations

484 (*ERBB2* p.S310F) are detected in original patient's tumor samples (lymph node  
485 metastasis: LN), PDX (G1), and PDX (G2). B, Sanger sequencing results. An identical  
486 *ERBB2* mutation is detected in the patient's primary tumor.

487

488 **Figure 4. HER2-targeted therapies suppress the tumor growth of EMPD-PDX-H1**  
489 **harboring the *ERBB2* S310F mutation.**

490 Tumor-bearing NOD/Scid mice were randomized into no therapy, lapatinib 100  
491 mg/kg/day orally (A, B), trastuzumab 10 mg/kg intraperitoneally twice a week (C, D),  
492 or a combination of these two agents (E, F). Green arrowheads indicate the injection of  
493 trastuzumab. Tumor volumes and weights were calculated and analyzed as indicated in  
494 Materials and Method. The results are presented as means, with the error bars  
495 representing the SD from the mean. All comparisons were statistically significant  
496 between the following groups: combo, trastuzumab or lapatinib versus no therapy.

497

498 **Figure 5. EMPD-PDX-H1 are sensitive to cytotoxic agents, including eribulin and**  
499 **docetaxel.**

500 Treatment experiments of cytotoxic agents using EMPD-PDX-H1. Tumor-bearing  
501 NOD/Scid mice were randomly treated with one of following injections: docetaxel at 20  
502 mg/kg once a week (A, B), eribulin at 1.5 mg/kg once a week (C, D), eribulin at 0.45

503 mg/kg (E, F) or sterile PBS once a week (control). The results are presented as means,  
504 with the error bars representing the SD from the mean. All comparisons are statistically  
505 significant between the following groups: the docetaxel group or the eribulin groups  
506 versus the control,  $P < 0.001$ . Blue, green, and red arrowheads indicate the injection of  
507 docetaxel, eribulin 1.5 mg/kg or eribulin at 0.45 mg/kg, respectively.

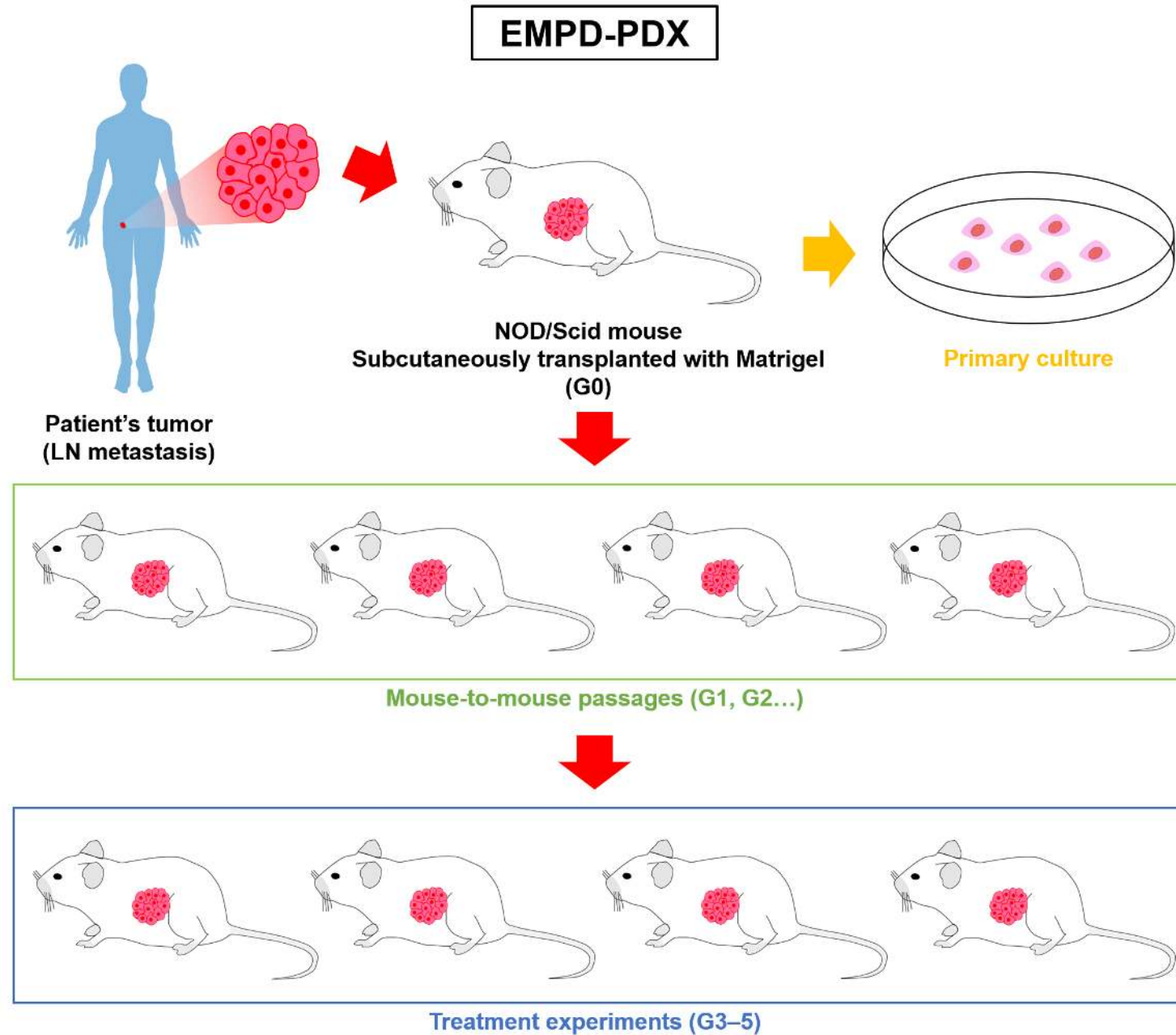
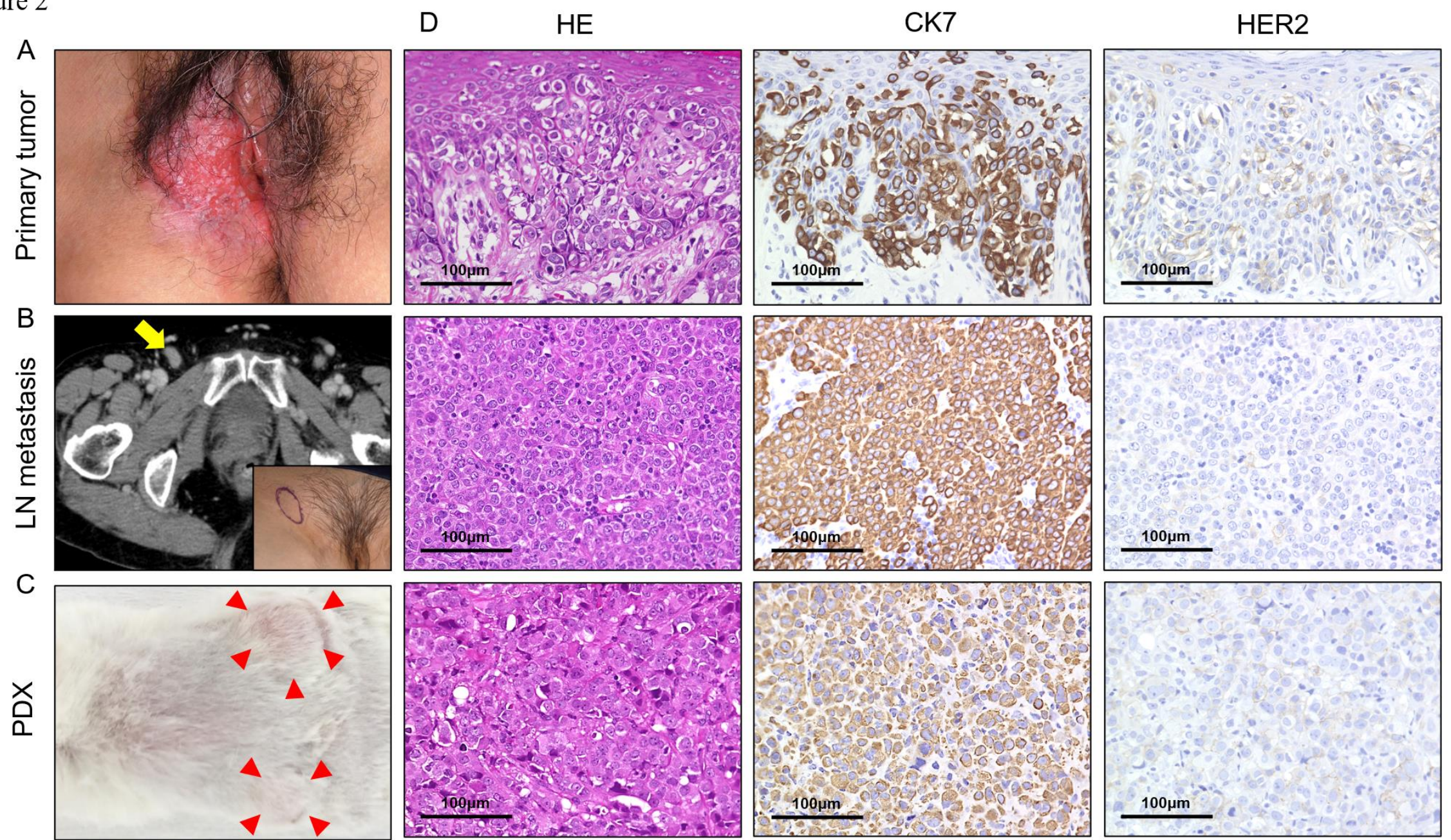




Figure 2

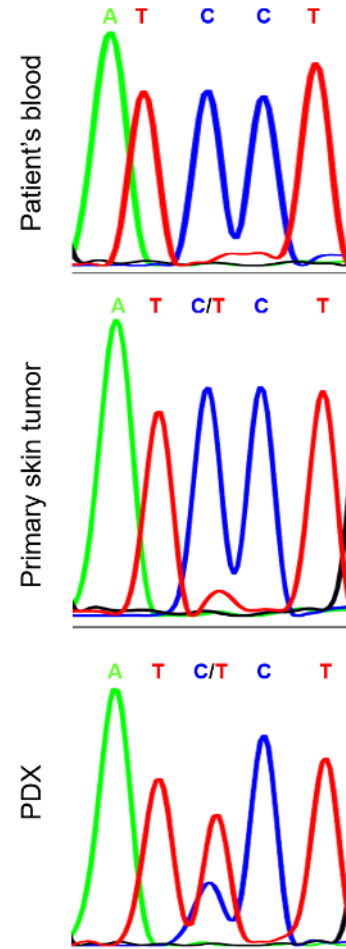


A

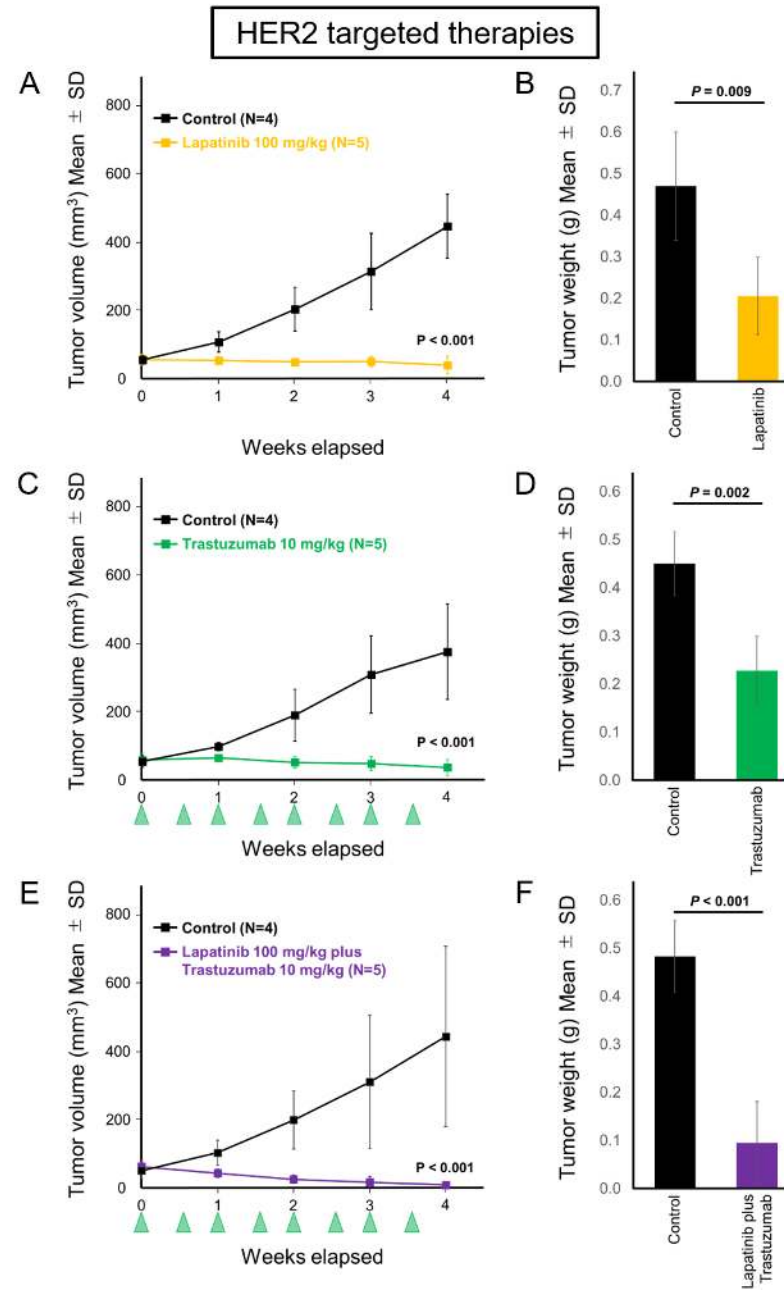
Sample characteristics	Major gene alterations (VAF, %)
Patient's blood	None
Patient's LN	<i>ERBB2</i> S310F (51.6%)
PDX (G1)	<i>ERBB2</i> S310F (70.7%)
PDX (G2)	<i>ERBB2</i> S310F (68.5%)

VAF: variant allele frequency

B *ERBB2* S310F (c.929C>T)



Maeda et al.  
Figure 4



Maeda et al.  
Figure 5

